



HAL
open science

Double fluorescent knock-in mice to investigate endogenous mu-delta opioid heteromer subcellular distribution.

Lyes Derouiche, Stéphane Ory, Dominique Massotte

► **To cite this version:**

Lyes Derouiche, Stéphane Ory, Dominique Massotte. Double fluorescent knock-in mice to investigate endogenous mu-delta opioid heteromer subcellular distribution.. *NeuroMethods* volume 140, 2018. hal-02511619

HAL Id: hal-02511619

<https://hal.science/hal-02511619>

Submitted on 18 Mar 2020

HAL is a multi-disciplinary open access archive for the deposit and dissemination of scientific research documents, whether they are published or not. The documents may come from teaching and research institutions in France or abroad, or from public or private research centers.

L'archive ouverte pluridisciplinaire **HAL**, est destinée au dépôt et à la diffusion de documents scientifiques de niveau recherche, publiés ou non, émanant des établissements d'enseignement et de recherche français ou étrangers, des laboratoires publics ou privés.

1 **Title: Double fluorescent knock-in mice to investigate endogenous mu-delta opioid**
2 **heteromer subcellular distribution.**

3

4 Authors: Lyes Derouiche, Stéphane Ory and Dominique Massotte

5

6 Address:

7 Institut des Neurosciences Cellulaires et Intégratives, UPR 3212 CNRS, Strasbourg, France

8 Corresponding author:

9 Dominique Massotte

10 INCI UPR 3212 CNRS

11 5 rue Blaise Pascal

12 F-67084 Strasbourg cedex 03

13 France

14 Tel : +03 88 45 66 52

15 d.massotte@unistra.fr

16

17 Running title: Endogenous Mu-delta heteromer internalization

18

19 Key words: heteromers, opioid receptors, mu-delta, trafficking, primary neuronal culture,
20 GPCR

21

22 Number of words: 4943

23 Number of figures: 2

24 Number of tables: 1

25

26 **ABSTRACT**

27 The heteromerization of Mu (MOP) and delta (DOP) opioid receptors has been extensively
28 studied in heterologous systems. These studies demonstrated significant functional
29 interaction of MOP and DOP evidenced by new pharmacological properties and intracellular
30 signalling in transfected cells co-expressing the receptors. Due to the lack of appropriate
31 tools for receptor visualization, such as specific antibodies, the pharmacological and
32 functional properties of MOP-DOP heteromers in cells naturally expressing these receptors
33 remains poorly understood. To address endogenous MOP-DOP heteromer trafficking and
34 signalling in vivo and in primary neuronal cultures, we generated a double knock-in mouse
35 line expressing functional fluorescent versions of DOP and MOP receptors. This mouse
36 model has successfully been used to map the neuroanatomic distribution of the receptors
37 and to identify brain regions in which the MOP-DOP heteromers are expressed. Here, we
38 describe a method to quantitatively and automatically analyze changes in the subcellular
39 distribution of MOP-DOP heteromers in primary hippocampal culture from this mouse
40 model. This approach provides a unique tool to address specificities of endogenous MOP-
41 DOP heteromer trafficking.

42 **INTRODUCTION**

43 Opioid receptors belong to the subfamily of Class A G protein-coupled receptors (GPCRs).
44 Four subtypes of opioid receptors mu (MOP), delta (DOP), kappa (KOP) and nociceptin
45 (NOP) receptor respectively encoded by the *OPRM1*, *OPRD1*, *OPRK1* and *OPRL1* genes have
46 been identified several decades ago (for review see [1-3]). These seven transmembrane
47 domain receptors are functional in a monomeric form, but can also associate among
48 themselves to generate a larger assembly or with different subtypes of opioids or non-opioid

49 receptors. In the latter case, the new entity is called heteromer and may exhibit specific
50 functional properties.

51 In the case of the opioid system, MOP and DOP functional interactions are well documented
52 Among others, they are essential for the development of opiate tolerance [4,5]. Numerous
53 studies indicate that co-expression of the two receptors in heterologous systems promotes
54 the formation of MOP-DOP heteromers, which affects binding and signaling properties [6,7].
55 However, in spite of a growing body of evidence in favor of the presence of MOP-DOP
56 heteromers *in vivo*, the molecular mechanisms underlying functional interactions between
57 these two receptors remain poorly characterized[8]. This is mainly due to the lack of
58 appropriate tools, especially specific antibodies.

59 To deal with this issue and study MOP-DOP heteromers *in vivo*, we generated a double
60 fluorescent knock-in mouse line co-expressing DOP and MOP receptors respectively fused to
61 their C-terminus to the enhanced green fluorescent protein (DOP-eGFP) or mcherry (MOP-
62 mcherry). The DOP-eGFP and MOP-mCherry functional fusions allow highly specific and
63 simultaneous visualization of endogenously expressed receptors with subcellular resolution
64 and proved to be unique tools for neuroanatomical studies [9]. Mapping of MOP and DOP
65 receptors in the central and peripheral nervous systems indeed revealed MOP-DOP neuronal
66 co-expression in discrete neuronal networks essential for survival such as the nociceptive
67 pathway (see also mouse brain atlas at <http://mordor.ics-mci.fr/>). Specific targeting using the
68 fluorescent tags also revealed MOP-DOP physical proximity in the hippocampus providing
69 strong rationale for the existence of endogenous MOP-DOP heteromers [9]. In addition, the
70 double fluorescent knock-in mice represent unique tools to explore the dynamics of this

71 complex under physiological or pathological conditions and to characterize the functional
72 impact of MOP-DOP heteromers in the central and peripheral nervous system.

73 In this chapter, we describe optimized conditions for visualization of endogenous MOP-DOP
74 heteromers in primary hippocampal neurons obtained from the double fluorescent knock-in
75 mice. We also provide a protocol for automatic quantitative analysis of confocal images with
76 an open source software to determine changes in receptor subcellular localization. This
77 method allowed MOP-DOP heteromers monitoring and specific determination of their
78 intracellular fate upon pharmacological activation.

79 **MATERIAL AND METHODS**

80 **1. Animals**

81 Double knock-in mice co-expressing fluorescent DOP and MOP receptors were obtained by
82 crossing previously generated DOP-eGFP and MOP-mcherry knock-in mice. Briefly, DOP-
83 eGFP knock-in mice expressing the delta opioid receptor fused to its C-terminus to the eGFP
84 were generated by homologous recombination by inserting the eGFP cDNA into exon 3 of
85 the delta opioid receptor gene, in frame and 5' from the stop codon [10]. MOP-mcherry
86 knock-in mice expressing the mu opioid receptor fused to its C-terminus to the red
87 fluorescent protein mCherry were generated by homologous recombination following a
88 procedure similar to the one used for DOR-eGFP knock-in mice [9]. The construct transfected
89 into ES cells comprised a Gly-Ser-Ile-Ala-Thr linker followed by the cDNA sequence
90 encoding the fluorescent protein (eGFP or mcherry). For subsequent clone selection, a
91 resistance gene was included that corresponded to neomycin flanked by loxP sites for DOP-
92 eGFP or to hygromycin flanked by FRT sites for MOP-mcherry (Figure 1). The resistance
93 gene was removed by microinjection of a plasmid expressing the recombinase. Blastocysts

94 were implanted in pseudo gestant BalbC females. Chimeric mice were crossed with C57Bl6/J
95 mice to obtain F1 heterozygous generation. Heterozygous animals were crossed to generate
96 mice homozygous for *Oprd1*-eGFP or *Oprm1*-mcherry that are fertile and develop normally.
97 Double knock-in animals were obtained by crossing the single knock-in mouse lines. The
98 genetic background of all mice was C57/BL6/J; 129svPas (50:50 %).

99 Mice were housed in animal facility under controlled temperature (21 ± 2 °C) and humidity
100 (45 ± 5 %) on a 12-h dark–light cycle with food and water ad libitum. All experiments were
101 performed in accordance to the European legislation (directive 2010/63/EU acting on
102 protection of laboratory animals) and the local ethical committee.

103 2. Primary hippocampal culture

104 2.1. Material and reagents:

- 105 • Double knock-in new born mice pups (P0-P3).
- 106 • 70% ethanol solution
- 107 • MilliQ water (autoclaved, or sterile filtered 0.22µm).
- 108 • Borate buffer (*see setup and procedures*)
- 109 • Poly-L-lysine hydrobromide (Sigma cat. No. P2623)
- 110 • 13 mm coverslips (Sigma, cat. no. P6407) coated with Poly-L-lysine (*see setup and*
111 *procedure*)
- 112 • 24-well sterile culture plates (Falcon cat. no. 353047).
- 113 • Pasteur pipets (flamed at the extremity, cotton plugged and autoclaved).
- 114 • Hibernate minus phenol red (BrainBits SKU: HAPR)
- 115 • Papain (Worthington, cat. no. LS003126)

- 116 • Dulbecco's Modified Eagle's Medium (DMEM) with 4.5g glucose (GIBCO, cat. no.
117 71966-029)
- 118 • Neurobasal A (GIBCO, cat. no. A13710-01)
- 119 • Foetal Calf Serum FCS heat inactivated. **Caution:** *test several batches to determine the*
120 *best one for your culture conditions.*
- 121 • Glutamax™ (GIBCO, cat. no. 35050061)
- 122 • L-glutamine (GIBCO, cat. no. 25030081)
- 123 • Penicillin-streptomycin (P/S) (cat. no. 15140122)
- 124 • DNase (Sigma cat. no. DN25).
- 125 • B27 supplement (GIBCO, cat. no. 17504044)
- 126 • Trypan blue solution (Sigma, cat. no. T8154)
- 127 • Paraformaldehyde 32% solution diluted to 4% before use (*see setup and reagents*).
- 128 • Phosphate buffer saline (PBS). (Sigma-Aldrich, cat. no. P5493)
- 129 • Cell strainer 70µm (Falcon, cat. no. 352350)

130 2.2. Setup and procedures

131 **2.2.1. Borate buffer:** dissolve boric acid 1,24g and Sodium tetraborate (borax) 1,9g in 400ml
132 MilliQ H₂O. pH should be 8.4. Sterile filter (0.22µm) before use. **Caution:** *borax is a hazardous*
133 *substance, manipulate cautiously and eliminate waste according to the safety rules fixed by your*
134 *institution/government.*

135 **2.2.2. Coverslips sterilisation and coating:** put coverslips in a 100-mm petri dish, sterilise
136 in 70% ethanol during 2 h under gentle agitation, let dry completely under laminar flow, and
137 transfer to culture plates. Rinse once with MilliQ water. Coat coverslips with poly-L-lysine
138 25µg/ml final concentration in borate buffer; incubate at 37°C for 2h to overnight. Rinse 3
139 times with sterile water and pre-warm in DMEM medium. Coated coverslips may be

140 prepared several days before use, dried in the laminar flow hood and kept sealed at 4°C for
141 up to 1 month.

142 **2.2.3. Dissection medium:** Prepare 5 mL of of ice cold Hibernate supplemented with 1X P/S
143 and 0.5nM glutamax per animal and transfer 0.5 mL dissection medium in a 15-mL
144 centrifugation tube per animal (2 hippocampi).

145 **2.2.4. Enzyme solution:** prior to dissection, prepare a fresh solution of Papain at 40U/mL
146 concentration in Hibernate medium, incubate 5 minutes at 37°C in a water bath then keep on
147 ice until use. Prepare 0.5 mL per animal (2 hippocampi).

148 **2.2.5. Plating medium:** Prepare 12 mL DMEM medium supplemented with 4.5 g/l glucose
149 + 10% heat inactivated FCS + 2mM Glutamine + Pen/strep) per animal on the day of use.

150 **2.2.6. Growing medium:** Prepare 12 mL Neurobasal medium supplemented with 2% B27,
151 2mM glutamax, 0.5mM glutamine and 1X P/S per animal on the day of use.

152 **2.2.7. Phosphate-buffered saline (PBS):** prepare 1L 1X PBS working solution from 10X
153 stock solution by diluting with MilliQ water. Check the pH and adjust to 7.4 with 1M HCl or
154 1M NaOH solutions if needed. Sterile filter 0.22µm and keep at 4°C for up to 6 months.

155 **2.2.8. Fixation solution:** dilute paraformaldehyde (PFA) 32% solution to 4% final
156 concentration in PBS 0.1M, adjust pH to 7.4 if needed. Prepare 500µl per well for use in 24-
157 well plate. Keep up to 5 days at 4°C and up to 6 months at -20°C. *Caution: PFA a hazardous*
158 *highly toxic substance, manipulate under flow hood and eliminate waste according to the safety rules*
159 *fixed by your institution/government.*

160 **2.3. Dissection and culture procedures**

161 **2.3.1. Dissection and cell dissociation**

162 Decapitate pups. Transfer the head in a 33mm petri dish with 1.5 mL ice cold dissection
163 medium and isolate the brain. Place the isolated brain in a new 33mm petri dish with 1.5mL

164 ice cold dissection medium. Remove the meninges, dissect to isolate the two hippocampi and
165 keep them in 0.5mL dissection solution in a 15 mL-tube in ice. Add 0.5 mL of papain solution
166 per tube to 0.5 mL dissection medium (1mL final / 2 hippocampi). Place tubes in a water bath
167 at 37°C for 30 minutes with gentle shaking every 5-10 minutes. 5-10 minutes before digestion
168 ends, add DNase at a final concentration of 1mg/mL.

169 Remove papain solution by decantation, add 1mL of Hibernate, and triturate with Pasteur
170 pipet until the tissue is completely dissociated (about 15 to 20 times up-and-down are
171 sufficient) (*see note 1*). Centrifuge at 1000g for 5 minutes at 22°C. Remove the supernatant,
172 add 1mL plating medium to resuspend cells (3 to 5 gentle up-and-down with Pasteur pipet).
173 Filter the cell suspension through a 70µm-cell strainer to remove any residual aggregates.
174 Count cells by diluting 20µl of cell suspension in 80µl of 1:10 Trypan blue solution diluted in
175 PBS. Place 20µl of this solution in a cell counting chamber and count cells excluding Trypan
176 blue (viable cells) only.

177 **2.3.2. Plating and feeding**

178 Prewarm poly-L-Lysine coated plates in DMEM medium at 37°C. Remove DMEM and plate
179 cells in 24-well plates at a density of 80 000 to 100 000 cells per well in a final volume of 500
180 µL.

181 Incubate in a humid incubator at 37°C and 5% CO₂ and allow cells to adhere to the bottom of
182 plates during one hour. Remove the plating medium by aspiration, rinse once with 500µl of
183 prewarmed Neurobasal A medium, then add 500µl of growing medium and return back to
184 the incubator. Let cells grow during at least twelve days with half of the medium replaced
185 every four to five days.

186 **3. Processing and pharmacological treatments**

187 Pharmacological treatments should be realized between DIV 12 and DIV 15 after plating (*see*
188 *note 2*). Ligands are added in a volume not exceeding 10% of the culture medium volume.
189 Incubate cells during the appropriate time. At the end of the pharmacological treatment,
190 remove the plate from the incubator and immediately place on ice, carefully aspirate the
191 medium and wash twice with ice cold sterile filtered PBS. Remove PBS and add 500 μ L of
192 PFA 4% in ice cold PBS and incubate during 20 minutes on ice. Remove PFA and rinse twice
193 with ice cold PBS and proceed to immunostaining or keep sealed with Parafilm in 500 μ L PBS
194 at 4°C up to 30 days (*see note 3*).

195 **4. Immunocytofluorescence (ICF):**

196 **4.1. Material and reagents**

- 197 • Phosphate buffer Saline 0.1M, pH 7.4.
- 198 • Normal Goat Serum (NGS) (Sigma cat. no. S26)
- 199 • Tween20 (Euromedex cat. no. 2001-B)
- 200 • Primary and secondary antibodies (see table 1)
- 201 • ProLong™ Gold Antifade Mounting medium (Molecular Probes cat. no. P36935).
- 202 • DAPI (Sigma cat. no. D9542)
- 203 • Finepoint Forceps (Rubis Switzerland cat.no.1K920)
- 204 • Microscope glass slides.

205 **4.2. Setup and reagents**

206 4.2.1. **PBS Tween 20 solution (PBST):** add 0.2% (V:V) of Tween 20 solution to 1X PBS
207 solution (*see section 1.2.7*) , mix vigorously to complete dissolution and keep at 4°C. Bring at
208 room temperature before use.

209 4.2.2. **Blocking solution:** add 5% of Normal Goat Serum (NGS) to the PBST solution.

210 Prepare the day of use.

211 4.3. **Method**

212 Incubate fixed cells in 250 μ L of blocking solution for one hour under gentle agitation at

213 room temperature (20-22°C). Then remove the blocking solution by aspiration and incubate

214 2h at RT or overnight at 4°C with primary antibodies in blocking solution (250 μ L/well)

215 under gentle agitation. Wash three times in PBST and incubate for two hours protected from

216 light with specific secondary antibodies diluted in blocking solution (Table 1) (250 μ L/well).

217 Wash three times in PBST, incubate 5 minutes in DAPI solution (1 μ g/mL in PBS) for nuclei

218 staining and then wash three times in PBS followed by 1 wash in MilliQ H₂O. Remove

219 coverslips from wells with finepoint Forceps, let coverslips dry completely at room

220 temperature protected from light and mount on glass slides with ProLong™ Gold Antifade

221 mounting medium. Keep for up to one year at -20° protected from light.

222 5. **Confocal microscope**

223 Images were acquired with a laser-scanning confocal microscope Leica SP5 using 63X /NA

224 1.4 oil immersion lens and X5 numerical zoom. The Pinhole was adjusted to 1 airy Unit and

225 the gain was adjusted without offset for each filter on a specific scanning plan allowing

226 specific acquisition without saturation. Image acquisition was performed according to

227 Nyquist parameters in XY with an average frame of 3 in a sequential scan mode to avoid

228 cross talk between different wavelengths. Z-stacks were obtained by scanning the whole

229 neuron thickness with step of 1 μ m in z.

230 6. **Image analysis with ICY open source software**

231 Confocal images were analyzed with ICY software (<http://icy.bioimageanalysis.org/>).
232 Quantification was performed on a single plane extracted from a z-stack. The analysis
233 combined two sequential steps. The first one consists in isolating each neuron to define
234 regions of interest (ROI). The second one involves the detection of the spots in each channel
235 and the determination of the amount of co-localisation in each ROI.

236 **6.1. ROI definition**

237 Each neuron was carefully delineated using the “free-hand area” tool. This initial ROI is
238 filled with the “fill holes in ROI” plugin to define the total cell area (ROI_{total}). ROIs were then
239 processed to generate two ROIs corresponding to the cell periphery and the cytoplasm
240 (detailed protocol available online <http://icy.bioimageanalysis.org/>). Based on staining in basal
241 conditions, we estimated that most of the plasma membrane staining was found over an 8
242 pixels thickness. Therefore, we automatically eroded with the “Erode ROI” plugin the ROI
243_{total} by 8 pixels and subtracted this new ROI (ROI_{cyto}) to ROI_{total} to obtain a ROI
244 corresponding to the cell periphery (ROI_{peri}).

245 **6.2. Spots detection and co-localisation**

246 To detect specific signal in each ROI, we used the “spot detector” plugin which rely on the
247 wavelet transform algorithm [11]. By carefully setting the sensitivity threshold and the scale
248 of objects to detect, it allows detection of spots even in images with low signal to noise ratio.
249 In our conditions, the sensitivity threshold was fixed between 50 and 60 % and the scale of
250 objects set at 2 (pixel size 3) for mu and delta receptors. Once parameters were defined,
251 images were images were processed with the tool “protocol” in Icy which is a graphical
252 interface for automated image processing. Data including the number of spots detected in
253 each channel and ROIs, the number of co-localized objects and the ROI area were

254 automatically collected in excel files. Objects were considered co-localized if the distance of
255 their centroid was equal to or less than 3 pixels. The protocol is available online
256 (*NewColocalizer with binary and excel output v1_batch.xml*). To obtain histograms we calculated
257 object densities for each receptor reported to the surface of each ROI. Membrane to
258 cytoplasm density ratios were calculated to illustrate the subcellular distribution of each
259 receptor. The extend of co-localisation was calculated according to the following formula for
260 each ROI [% *colocalisation* = $100X \left(\frac{\text{colocalised MOP and DOP objects}}{\Sigma(\text{detected MOP and DOP objects})} \right)$].

261 7. Statistical analysis

262 Statistical analyses were performed with Graphpad Prism V7 software (GraphPad, San
263 Diego, CA). Normality of the distributions and homogeneity of the variances were checked
264 before statistical comparison to determine appropriate statistical analysis. In our case, data
265 were not normally distributed and the non-parametric Mann Witney test was used to
266 compare receptor densities in the plasma membrane and cytoplasm in basal conditions or
267 after agonist treatment. The extend of receptor co-localisation was compared using two-way
268 ANOVA with repeated measures followed by post-hoc Sidak's test for multiple
269 comparisons. Basal group was compared to agonist treated group (first factor) within
270 cytoplasm and plasma membrane localisation (second factor).

271 RESULTS AND DISCUSSION

272 In this chapter, we have presented an optimized method for monitoring the subcellular
273 distribution of endogenous MOP and DOP receptors. To this aim, we combined the use of a
274 genetically modified mouse line co-expressing functional fluorescently tagged receptors,
275 optimized primary neuronal culture protocol and automatic quantitative analysis of confocal

276 images with an open source software. Importantly, the image analysis procedure can be
277 easily implemented in any laboratory since data processing does not require extensive
278 mathematical developments or program writing with specialized software.

279 **Individual distribution of MOP and DOP receptors**

280 High magnification confocal images analyzed as single focal plan revealed discontinuous
281 and punctate distributions for DOP-eGFP and MOP-mCherry that were predominantly
282 located at the cell surface in basal conditions (Figure 2-A). Images also revealed a perinuclear
283 cytoplasmic localization of both receptors that likely correspond to receptor stock in the
284 endoplasmic reticulum. These observations were consistent with data from the literature
285 describing a predominant and membrane localization of DOP [10,12] and MOP [13] but also
286 substantial localization in perikarya [10].

287 Quantification using the ICY software indicated a higher density of fluorescent objects at the
288 cell surface for both MOP and DOP receptors (Figure 2-B) that was three times higher
289 compared to the cytoplasm (Fig. 2-C). Activation by the MOP-DOP agonist CYM51010 led to
290 the appearance of high intensity punctate structures in the cytoplasmic and a dramatic
291 decrease in the plasma membrane labelling of both receptors (figure 2-A). Accordingly, the
292 ratio corresponding to the density of fluorescent objects density at the plasma membrane
293 compared to the cytoplasm dropped dramatically from 3 to 1 for both MOP and DOP
294 receptors which supports internalization of the two receptors in vesicle-like structures.

295 These results are in agreement with previous reports using the density of fluorescence to
296 estimate changes in DOPeGFP subcellular distribution *in vivo*. In these studies, the ratio of
297 fluorescence density between the plasma membrane and cytoplasm was about 1.5 in basal

298 conditions and significantly decreased following agonist stimulation [10,14]. We therefore
299 tested our quantification method using images of DOR-eGFP neurons in the hippocampus
300 acquired with similar parameters in confocal microscopy. Using the protocol described
301 above, we found that the density in DOP-eGFP objects under basal conditions was around 3
302 similar to our results in primary neuronal cultures. We also established that this value
303 corresponded to a ratio in fluorescence density between the plasma membrane and the
304 cytoplasm of about 1.7, similar to previously reported ratios [10]. Moreover, we quantified
305 the ratio of fluorescence density between the plasma membrane and the cytoplasm using the
306 set of images used in Erbs et al 2016, and calculated a similar increase of about 10% in DOP-
307 eGFP expression at the plasma membrane after chronic morphine treatment in the neurons
308 of the hippocampus [15]. Altogether, these results fully validate the quantification method
309 developed using ICY software.

310 **Co-localization of MOP and DOP receptors and detection of MOP-DOP** 311 **heteromers**

312 Our analysis revealed substantial colocalization of MOP and DOP associated signals under
313 basal conditions. In fact, more than 22% of the MOP and DOP objects were co-localized
314 within the plasma membrane whereas cytoplasmic colocalization was fairly low (around
315 10%) (Figure 2-D). After selective MOP-DOP activation with the agonist CYM51010, the
316 cytoplasmic colocalization was increased by 87% to reach 18.7%. A two-fold decrease in the
317 percentage of MOP-DOP colocalization within the plasma membrane was also observed
318 after CYM51010 treatment (Figure 2-D). These observations support a view in which MOP
319 and DOP receptors remain associated upon specific activation of the heteromers and
320 undergo common intracellular fate.

321 It is however important to note, that due to the resolution limit of confocal microscopy,
322 MOP-DOP physical interaction has to be assessed by other experimental approaches such as
323 co-localization in electron microscopy or disruption of the physical contact by a
324 transmembrane peptide. The latter has been successfully performed for MOP-DOP receptors
325 *in vivo*. Indeed, a peptide corresponding to the MOP TM 1 or to the DOP second intracellular
326 loop in fusion with the cell transduction domain of the human immunodeficiency virus
327 (HIV) TAT protein interfered with MOP-DOP co-immunoprecipitation [16-18]. The recently
328 described proximity ligation assay [19] provides high spatial resolution and represents
329 another attractive option to address physical proximity.

330 In addition, the resolution of the images did not enable to distinguish the pool of receptors
331 associated to the plasma membrane from receptors located in the sub-membrane
332 compartment which represents another limitation of our analysis. Total internal reflection
333 fluorescence microscopy (TIRFM) would be required to differentiate the two compartments
334 and precisely monitor the first steps in receptor internalization.

335 MOPmcherry-DOPeGFP co-localisation studies could also be combined with identification of
336 the intracellular compartments using specific antibodies. This would enable for fine mapping
337 of the receptors in the vesicular structures and cellular compartments and would provide
338 detailed information on the intracellular fate of MOP-DOP heteromers.

339 **CONCLUSION**

340 Double knock-in mice represent unique tools to investigate endogenous MOP-DOP
341 neuroanatomical distribution but also to explore functional dynamics in physio-pathological
342 conditions. As described here, the use of double fluorescent knock-in mice combined with

343 confocal imaging and ICY software analyses enables easy quantification of receptor sub-
344 cellular distribution and co-localisation, hence specific MOP-DOP trafficking. Importantly,
345 the field of application of the method described here is not restricted to the study of MOP-
346 DOP heteromers but can be applied to address the heteromerization of any other pair of
347 GPCRs. Moreover, the analysis with the ICY software is not restricted to the study of
348 receptors but is widely applicable to monitor the co-localisation of any two objects detected
349 independently and can be applied to any type of high-resolution images.

350 NOTES

- 351 1- Cell dissociation is a critical step; if the trituration is too gentle, the tissue will not
352 dissociate, if too vigorous cells will break.
- 353 2- Because re-expression of DOP-eGFP and MOP-mCherry is only detectable from day
354 in vitro (DIV) 10 in primary neurons, pharmacological treatments should be
355 performed between DIV12 and DIV15 to ensure full expression of the receptors.
- 356 3- Paraformaldehyde fixation decreases the fluorescence intensity of eGFP and mCherry
357 and amplification by immunostaining is recommended. The DOP-eGFP construct can
358 also be used for *ex vivo* real-time imaging of receptor internalization by confocal
359 microscopy [10]. However, due to the low expression level of endogenous MOP
360 receptors and their weak expression at the plasma membrane in basal conditions,
361 real-time monitoring of MOP-mcherry remains presently below the detection limit.

362 ACKNOWLEDGMENTS

363 The authors would like to acknowledge the financial support of the Fondation pour la
364 Recherche Médicale (LPA20140129364). L. Derouiche was the recipient of an IDEX post-
365 doctoral fellowship of the University of Strasbourg.

366 **CONFLICT OF INTEREST**

367 The authors declare no conflict of interest

368 **REFERENCES**

- 369 1. Charbogne P, Kieffer BL, Befort K (2014) 15 years of genetic approaches in vivo for
370 addiction research: Opioid receptor and peptide gene knockout in mouse models of drug
371 abuse. *Neuropharmacology* 76 Pt B:204-217. doi:10.1016/j.neuropharm.2013.08.028
- 372 2. Pasternak GW (2014) Opioids and their receptors: Are we there yet?
373 *Neuropharmacology* 76 Pt B:198-203. doi:10.1016/j.neuropharm.2013.03.039
- 374 3. Civelli O (2008) The orphanin FQ/nociceptin (OFQ/N) system. *Results Probl Cell*
375 *Differ* 46:1-25. doi:10.1007/400_2007_057
- 376 4. Ong EW, Cahill CM (2014) Molecular Perspectives for mu/delta Opioid Receptor
377 Heteromers as Distinct, Functional Receptors. *Cells* 3 (1):152-179. doi:10.3390/cells3010152
- 378 5. Gendron L, Mittal N, Beaudry H, Walwyn W (2015) Recent advances on the delta
379 opioid receptor: from trafficking to function. *Br J Pharmacol* 172 (2):403-419.
380 doi:10.1111/bph.12706
- 381 6. Gomes I, Ijzerman AP, Ye K, Maillet EL, Devi LA (2011) G protein-coupled receptor
382 heteromerization: a role in allosteric modulation of ligand binding. *Mol Pharmacol* 79
383 (6):1044-1052. doi:10.1124/mol.110.070847

- 384 7. Fujita W, Gomes I, Devi LA (2014) Revolution in GPCR signalling: opioid receptor
385 heteromers as novel therapeutic targets: IUPHAR review 10. *Br J Pharmacol* 171 (18):4155-
386 4176. doi:10.1111/bph.12798
- 387 8. Massotte D (2015) In vivo opioid receptor heteromerization: where do we stand? *Br J*
388 *Pharmacol* 172 (2):420-434. doi:10.1111/bph.12702
- 389 9. Erbs E, Faget L, Scherrer G, Matifas A, Filliol D, Vonesch JL, Koch M, Kessler P,
390 Hentsch D, Birling MC, Koutsourakis M, Vasseur L, Veinante P, Kieffer BL, Massotte D
391 (2015) A mu-delta opioid receptor brain atlas reveals neuronal co-occurrence in subcortical
392 networks. *Brain Struct Funct* 220 (2):677-702. doi:10.1007/s00429-014-0717-9
- 393 10. Scherrer G, Tryoen-Toth P, Filliol D, Matifas A, Laustriat D, Cao YQ, Basbaum AI,
394 Dierich A, Vonesh JL, Gaveriaux-Ruff C, Kieffer BL (2006) Knockin mice expressing
395 fluorescent delta-opioid receptors uncover G protein-coupled receptor dynamics in vivo.
396 *Proc Natl Acad Sci U S A* 103 (25):9691-9696. doi:10.1073/pnas.0603359103
- 397 11. Olivo-Marin JC (2002) Extraction of spots in biological images using multiscale
398 products. *Pattern Recogn* 35 (9):1989-1996. doi:Pii S0031-3202(01)00127-3 Doi 10.1016/S0031-
399 3203(01)00127-3
- 400 12. Cahill CM, McClellan KA, Morinville A, Hoffert C, Hubatsch D, O'Donnell D,
401 Beaudet A (2001) Immunohistochemical distribution of delta opioid receptors in the rat
402 central nervous system: evidence for somatodendritic labeling and antigen-specific cellular
403 compartmentalization. *J Comp Neurol* 440 (1):65-84
- 404 13. Trafton JA, Abbadie C, Marek K, Basbaum AI (2000) Postsynaptic signaling via the
405 [mu]-opioid receptor: responses of dorsal horn neurons to exogenous opioids and noxious
406 stimulation. *J Neurosci* 20 (23):8578-8584

- 407 14. Faget L, Erbs E, Le Merrer J, Scherrer G, Matifas A, Benturquia N, Noble F,
408 Decossas M, Koch M, Kessler P, Vonesch JL, Schwab Y, Kieffer BL, Massotte D (2012) In vivo
409 visualization of delta opioid receptors upon physiological activation uncovers a distinct
410 internalization profile. *J Neurosci* 32 (21):7301-7310. doi:10.1523/JNEUROSCI.0185-12.2012
- 411 15. Erbs E, Faget L, Ceredig RA, Matifas A, Vonesch JL, Kieffer BL, Massotte D (2016)
412 Impact of chronic morphine on delta opioid receptor-expressing neurons in the mouse
413 hippocampus. *Neuroscience* 313:46-56. doi:10.1016/j.neuroscience.2015.10.022
- 414 16. He SQ, Zhang ZN, Guan JS, Liu HR, Zhao B, Wang HB, Li Q, Yang H, Luo J, Li ZY,
415 Wang Q, Lu YJ, Bao L, Zhang X (2011) Facilitation of mu-opioid receptor activity by
416 preventing delta-opioid receptor-mediated codegradation. *Neuron* 69 (1):120-131.
417 doi:10.1016/j.neuron.2010.12.001
- 418 17. Kabli N, Martin N, Fan T, Nguyen T, Hasbi A, Balboni G, O'Dowd BF, George SR
419 (2010) Agonists at the delta-opioid receptor modify the binding of micro-receptor agonists to
420 the micro-delta receptor hetero-oligomer. *Br J Pharmacol* 161 (5):1122-1136.
421 doi:10.1111/j.1476-5381.2010.00944.x
- 422 18. Xie WY, He Y, Yang YR, Li YF, Kang K, Xing BM, Wang Y (2009) Disruption of
423 Cdk5-associated phosphorylation of residue threonine-161 of the delta-opioid receptor:
424 impaired receptor function and attenuated morphine antinociceptive tolerance. *J Neurosci* 29
425 (11):3551-3564. doi:10.1523/JNEUROSCI.0415-09.2009
- 426 19. Dasiel O, Borroto-Escuela BH, Miles Woolfenden , Luca Pinton , Antonio Jiménez-
427 Beristain , Julia Ofl ijan , Manuel Narvaez , Michael Di Palma , Kristin Feltmann , Stfano
428 Sartini , Patrizia Ambrogini , Francisco Ciruela , Riccardo Cuppini , and Kjell Fuxe (2016) In
429 Situ Proximity Ligation Assay to Study and Understand the Distribution and Balance of

430 GPCR Homo- and Heteroreceptor Complexes in the Brain. Neuromethods, vol 110 Springer
431 Science+Business Media New York edn. doi:DOI 10.1007/978-1-4939-3064-7_9

432

433 **TABLE 1: Primary and secondary antibodies**

| Antigen | Antibody | Supplier reference | Dilution |
|-------------|-----------------------------------|-------------------------|----------|
| eGFP | Chicken IgY | AVES-GFP1020 | 1/1000 |
| mCherry | Rabbit IgG | Clontech-632496 | 1/1000 |
| Chicken IgY | Goat anti chicken Alexa Fluor 488 | Molecular Probes-A11039 | 1/2000 |
| Rabbit IgG | Goat anti rabbit Alexa Fluor 594 | Molecular Probes-A11012 | 1/2000 |

434

435 **FIGURE LEGENDS**

436 **Figure 1: Double Knock-in DOP-eGFP/MOP-mCherry mouse engineering. A)**

437 Construction of the DOP-eGFP mouse. A cDNA sequence corresponding to the eGFP cDNA,
438 and the FRT flanked neomycine (neo) cassette was inserted by homologous recombination
439 (HR) into the *Oprd1* locus. HR was followed Cre recombinase treatment in ES cells. **B)**

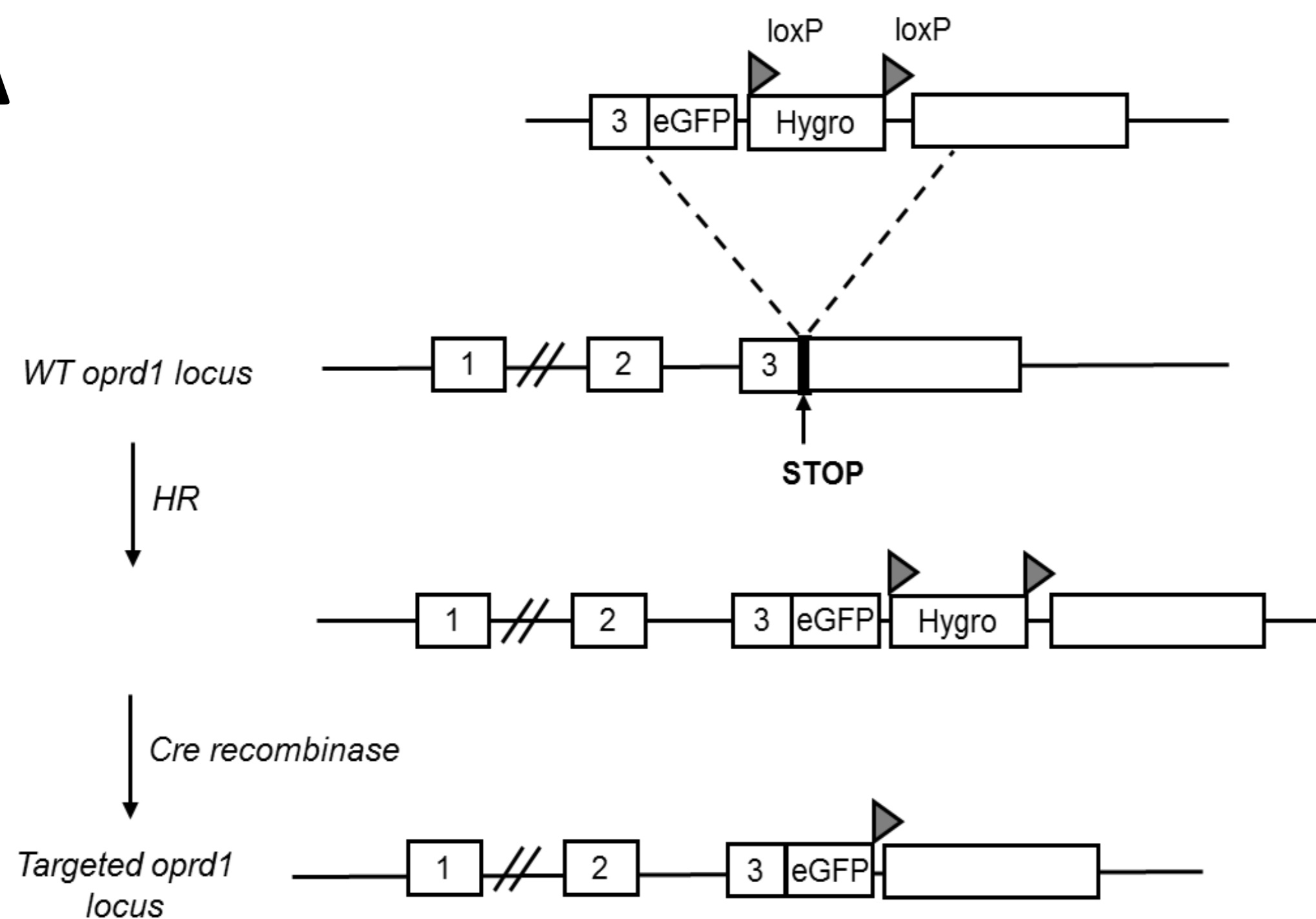
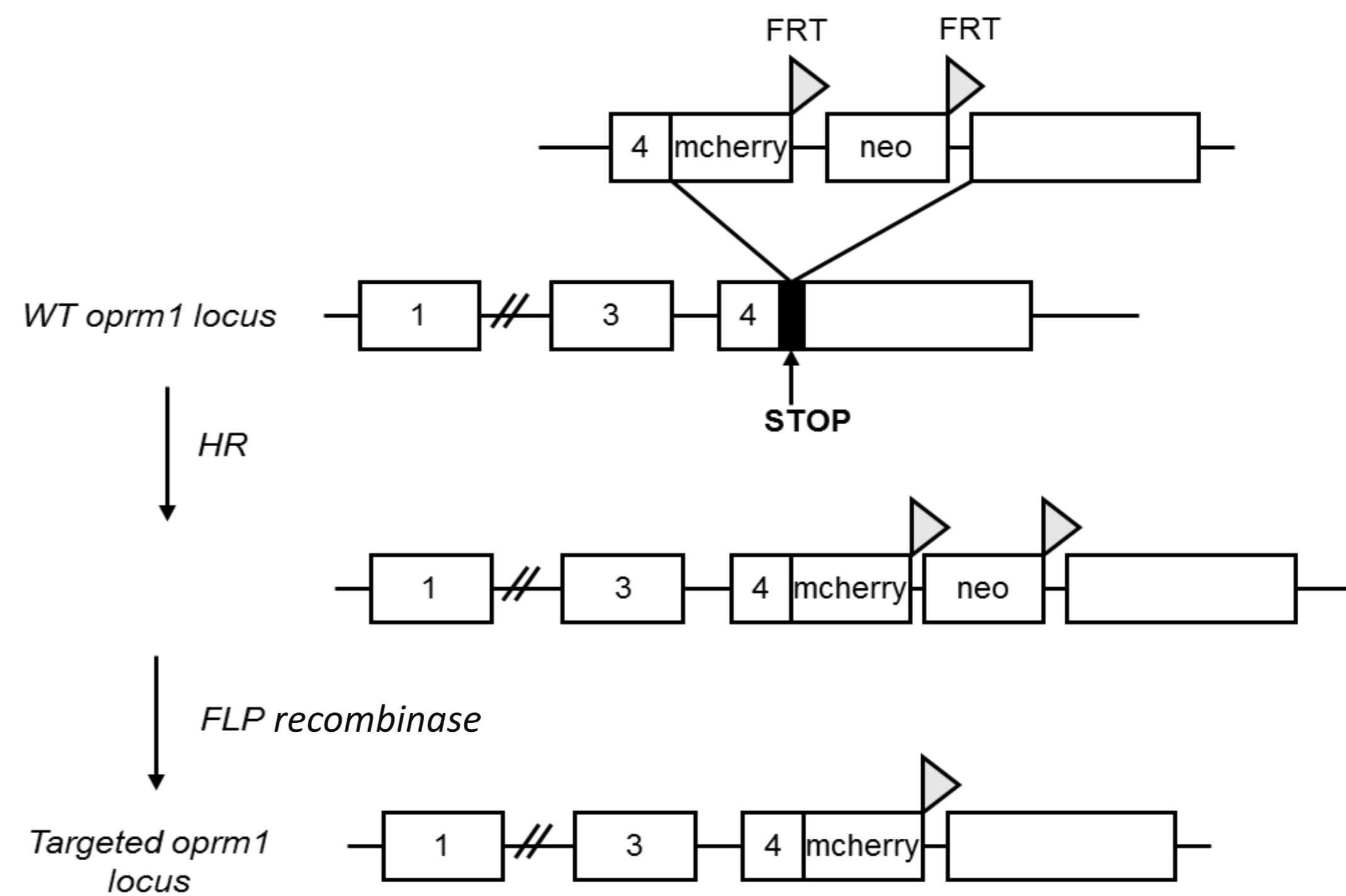
440 Construction of the MOP-mcherry mouse. A cDNA sequence corresponding mCherry
441 cDNA, and the loxP flanked hygromycine (hygro) cassette were inserted by HR to the *Oprm1*
442 locus. HR was followed by FRT recombinase treatment in ES cells. **(C)** Double knock-in mice
443 were obtained by crossing homozygote DOP-eGFP and MOP-mCherry mice.

444 **Figure 2: MOP-DOP heteromer visualisation and quantification. A)** Representative

445 confocal images illustrating MOP-mcherry and DOP-eGFP co-localisation in basal conditions

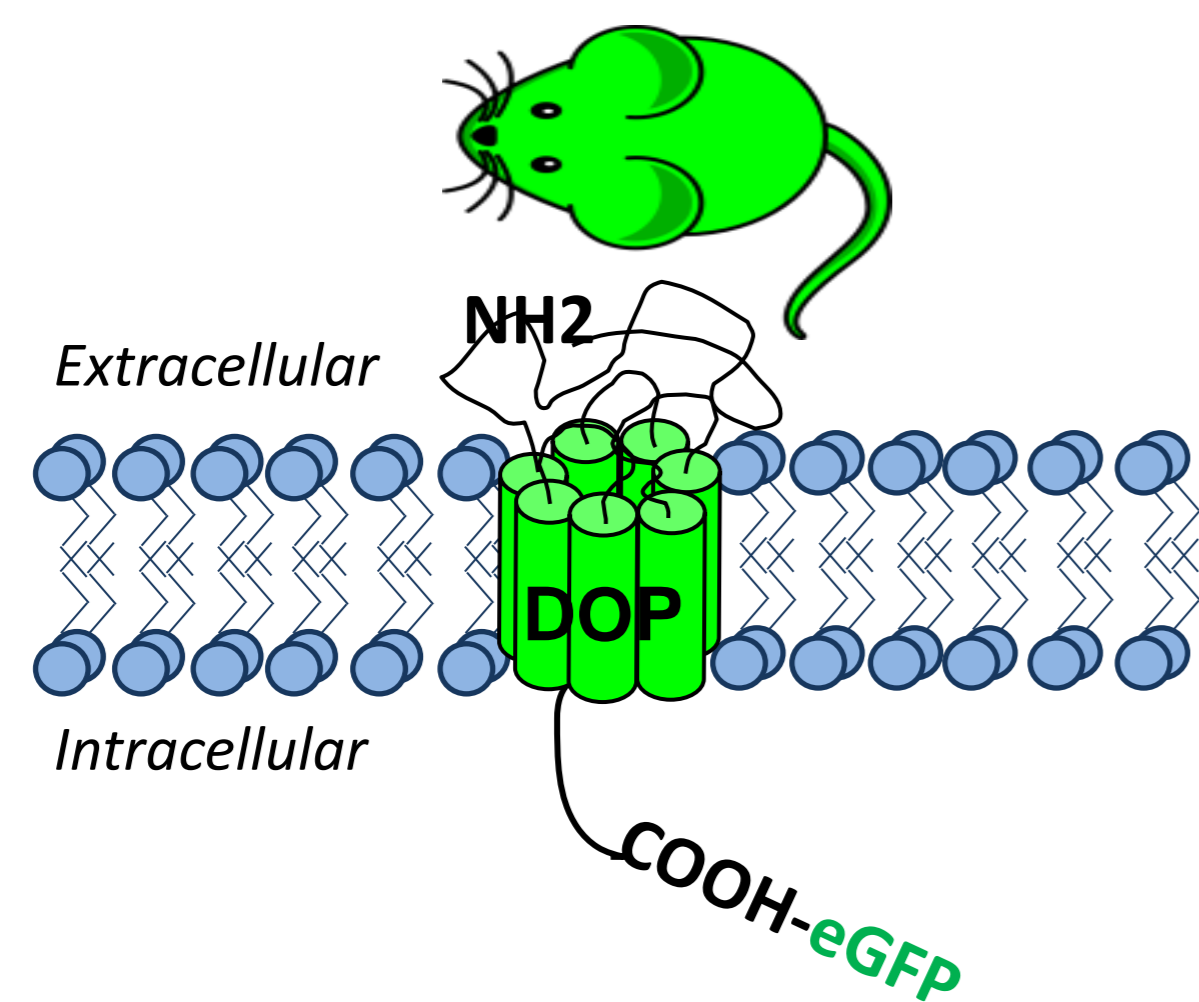
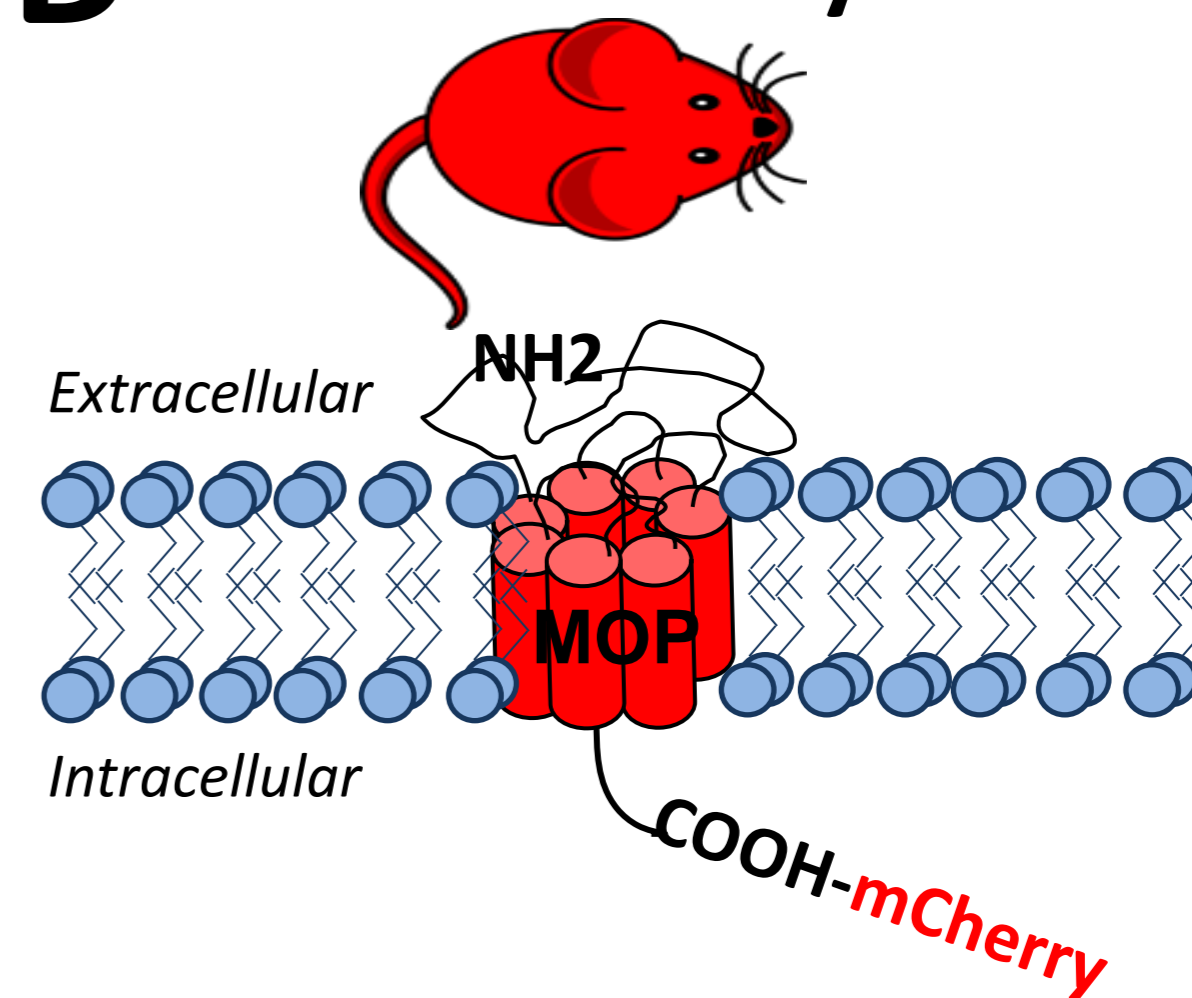
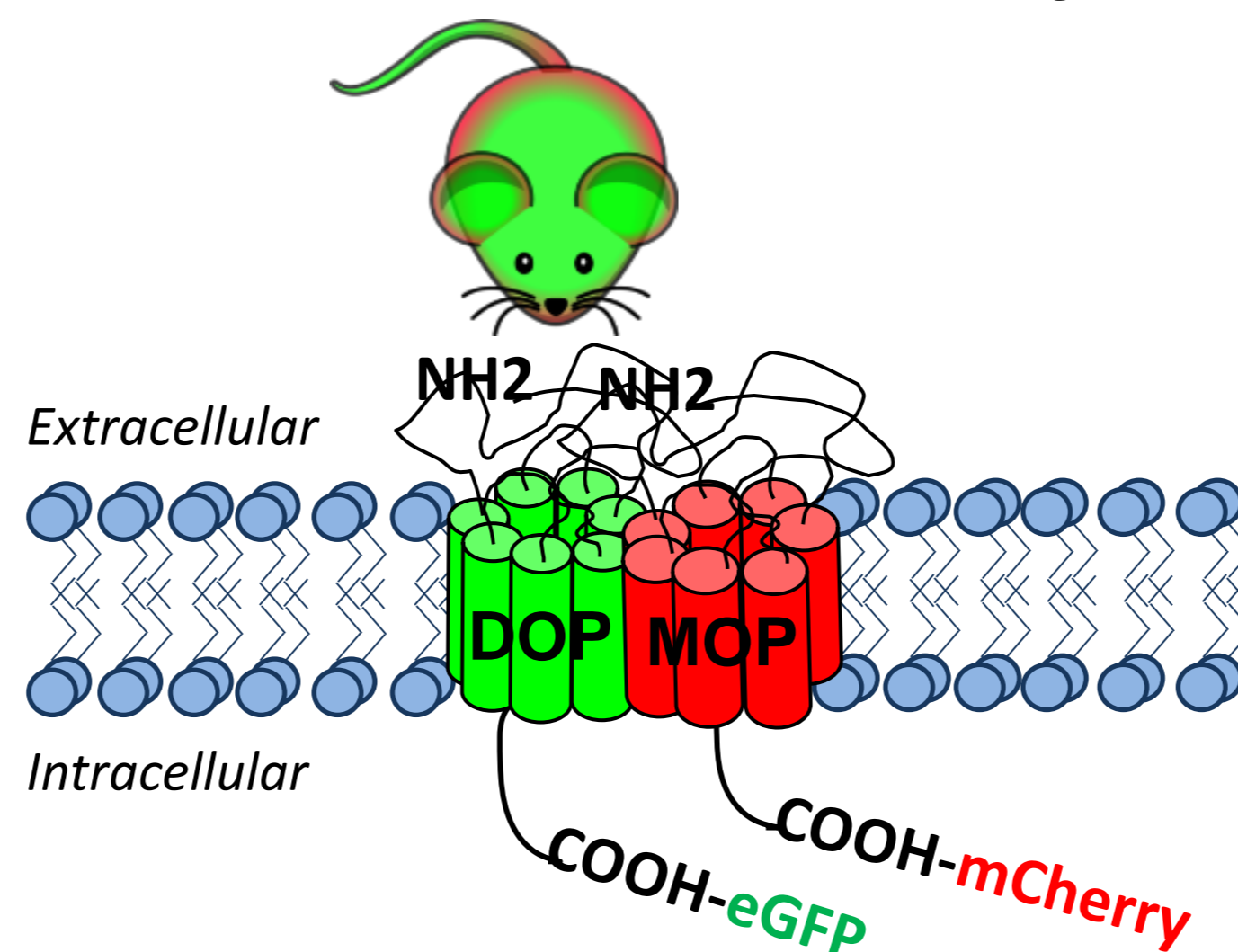
446 or after treatment during 60 minutes with the MOP-DOP agonist CYM51010 400nM. Scale
447 bar: 5µm. **B)** Image quantification with ICY software illustrating each receptor distribution.
448 In basal conditions, MOP and DOP densities are significantly higher in the plasma
449 membrane compared to cytoplasm. Mann Whitney test, *p-value <0.05. CYM51010 treatment
450 for 60 minutes led to changes in receptor subcellular distribution with no more statistical
451 difference in receptor densities between the plasma membrane and cytoplasm (Mann Whitney
452 test, p-value > 0.05). **C)** Changes in receptors distribution. Plasma membrane to cytoplasm
453 ratio of MOP or DOP spots densities in basal conditions or after with 400nM CYM51010 for
454 60 minutes reflects receptor redistribution. Mann Whitney test, ****p-value <0.001; **** p-value
455 <0.0001. **D)** Quantification of MOP-DOP co-localisation upon agonist activation with 400nM
456 CYM51010 for 60 minutes reveals MOP-DOP co-internalisation. Two-way ANOVA with
457 repeated measures, post-hoc Sidak's test. *p-value <0.05 for basal cytoplasm *vs* CYM51010
458 cytoplasm; **p-value <0.01 for basal membrane *vs* CYM51010 membrane. ### p-value <0.001
459 for basal membrane *vs* basal cytoplasm; NS: p-value >0.05 for CYM51010 membrane *vs*
460 CYM51010 cytoplasm.

461

A**B**

Adapted from Scherrer et al 2006 PNAS

Adapted from Erbs et al 2015 Brain Struct funct.

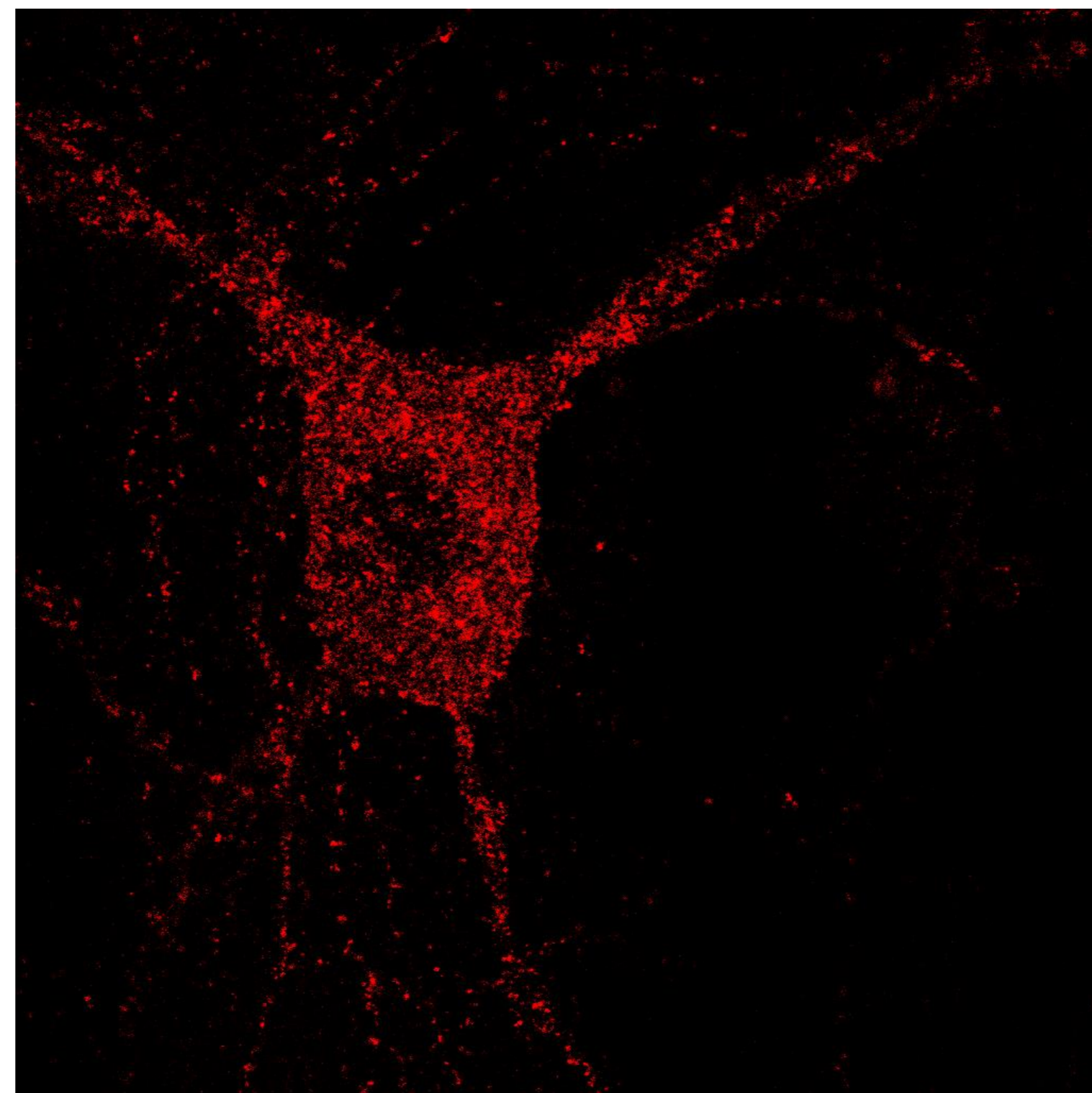
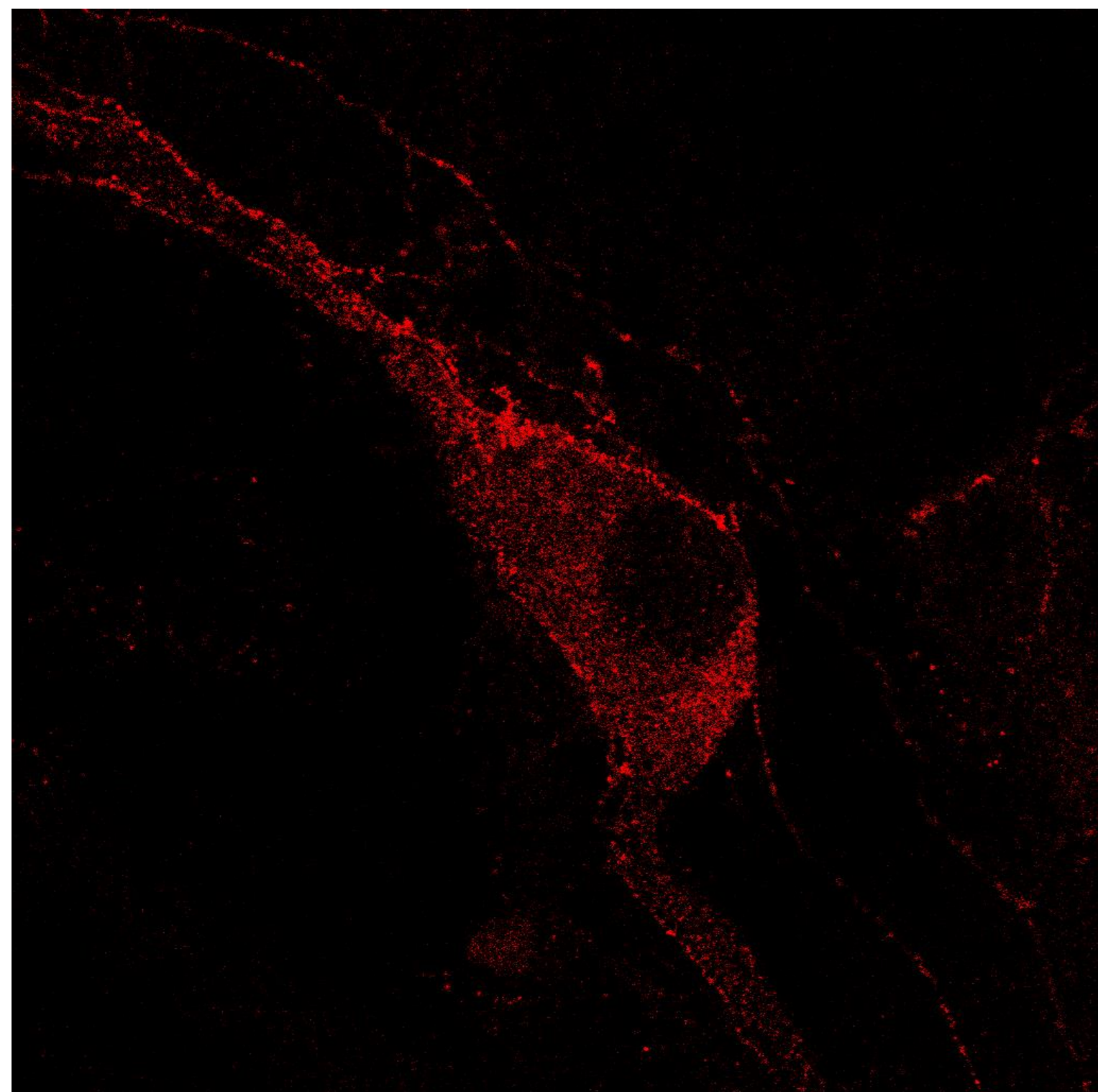
C DOP-eGFP/**D MOP-mCherry****E DOP-eGFP/MOP-mCherry**

A

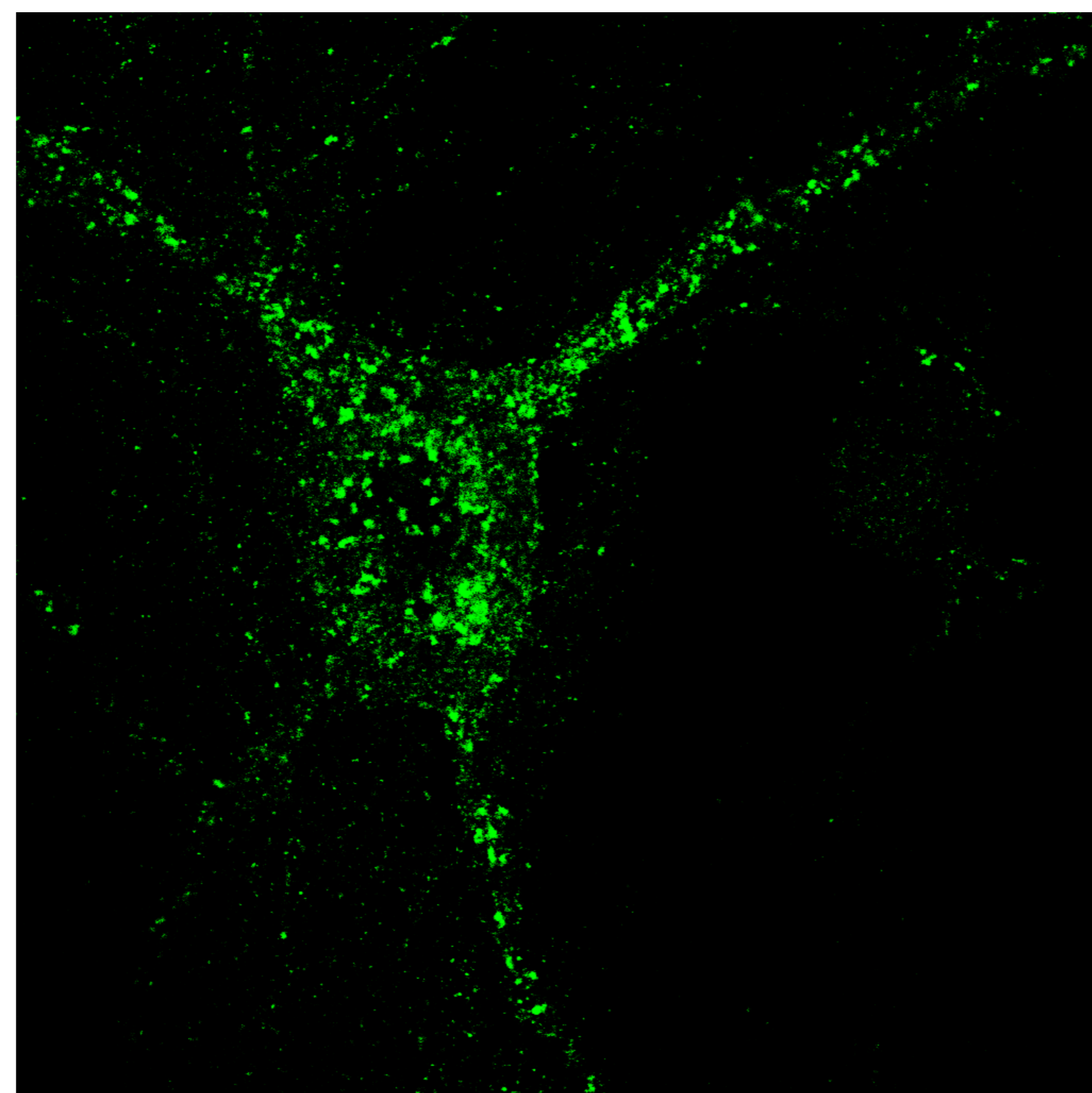
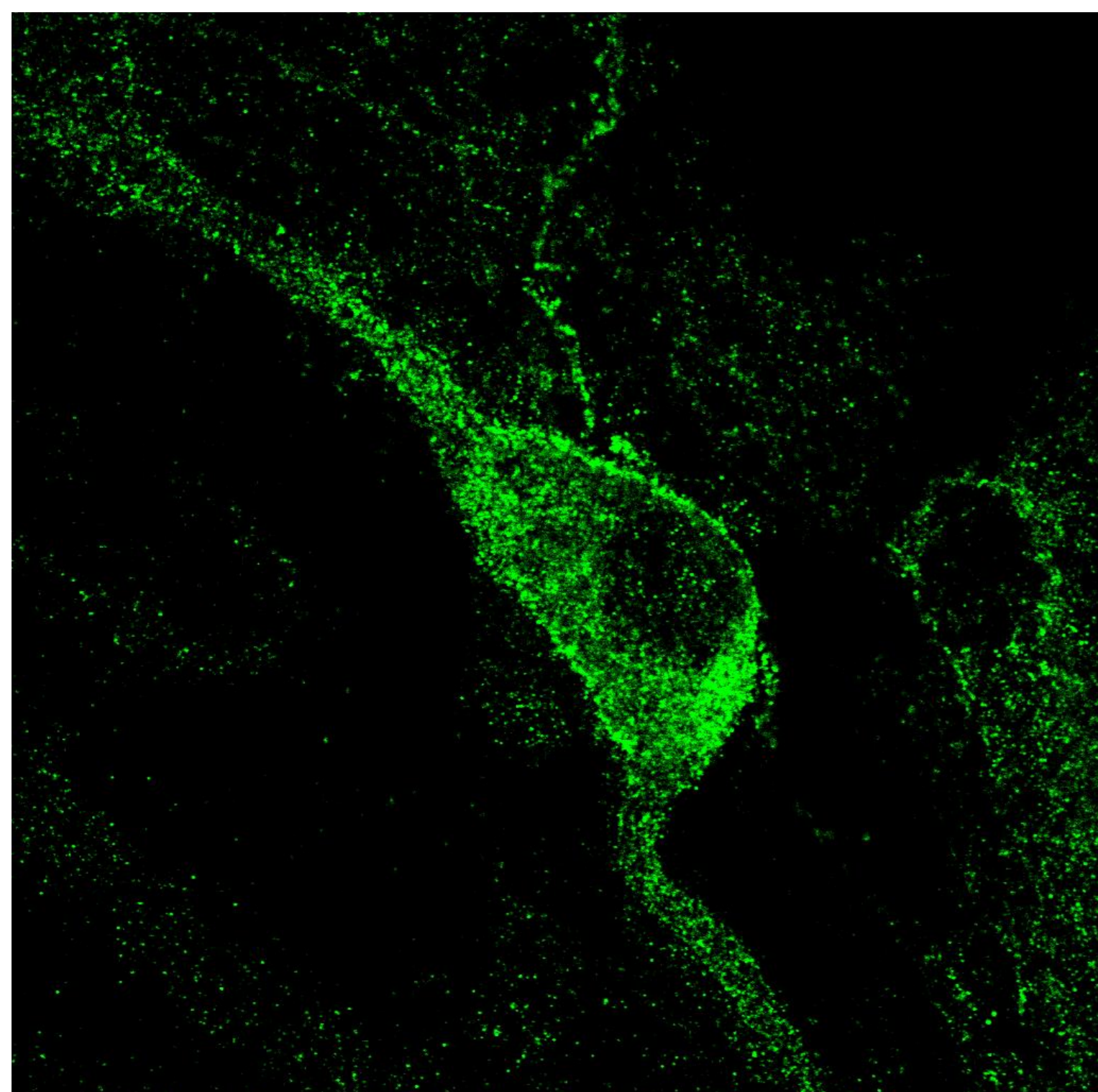
Basal

CYM51010 60 minutes

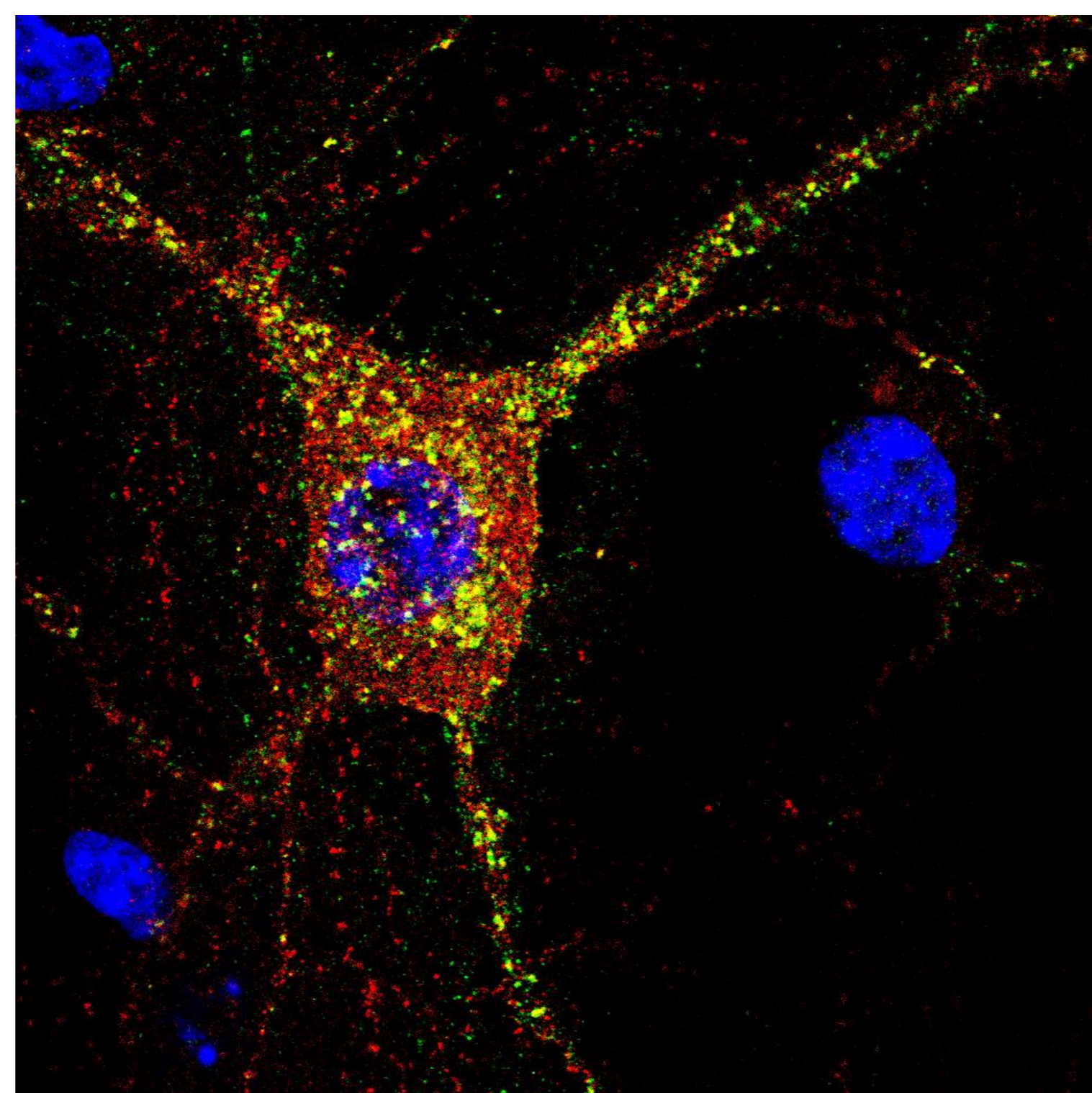
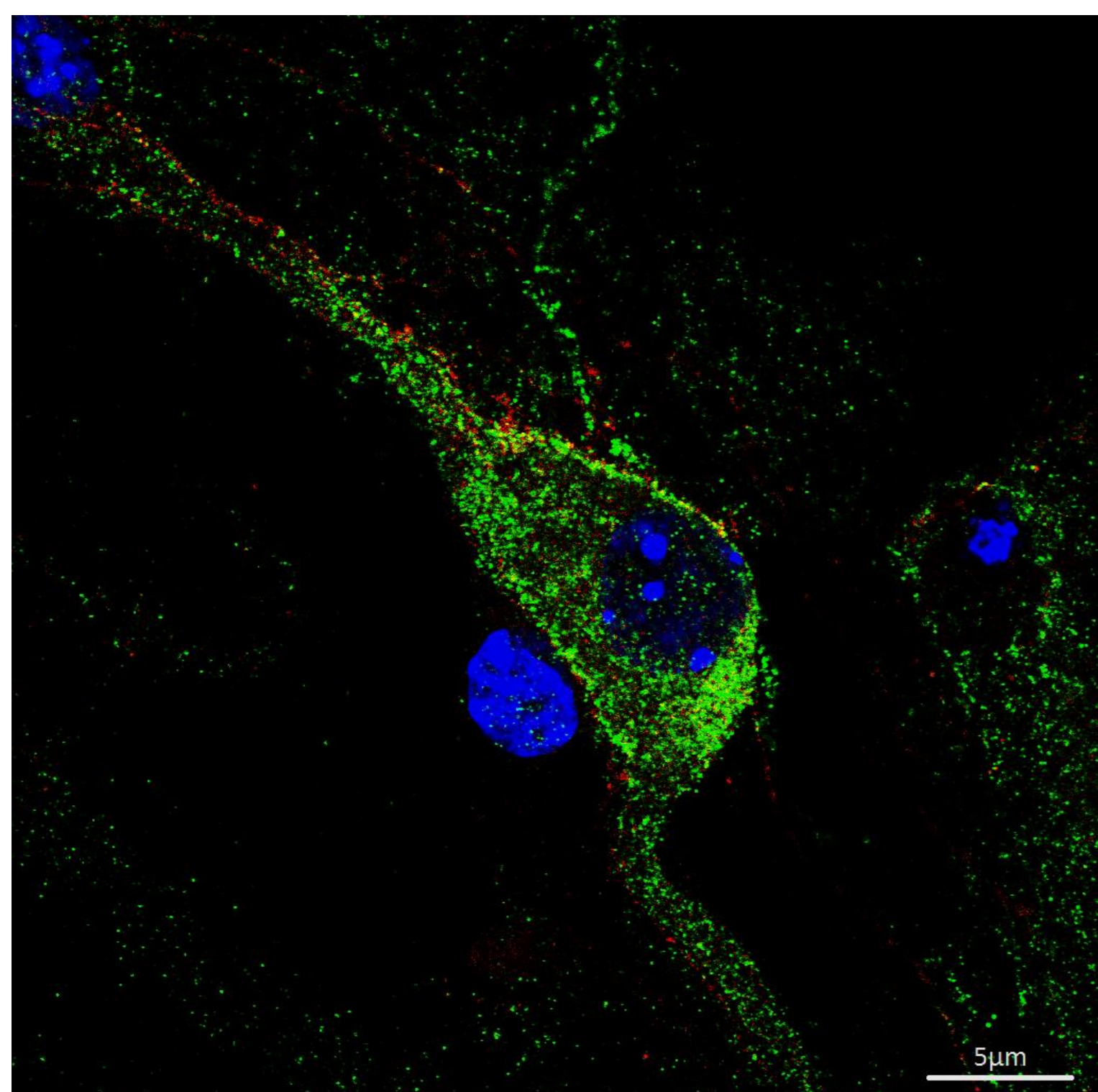
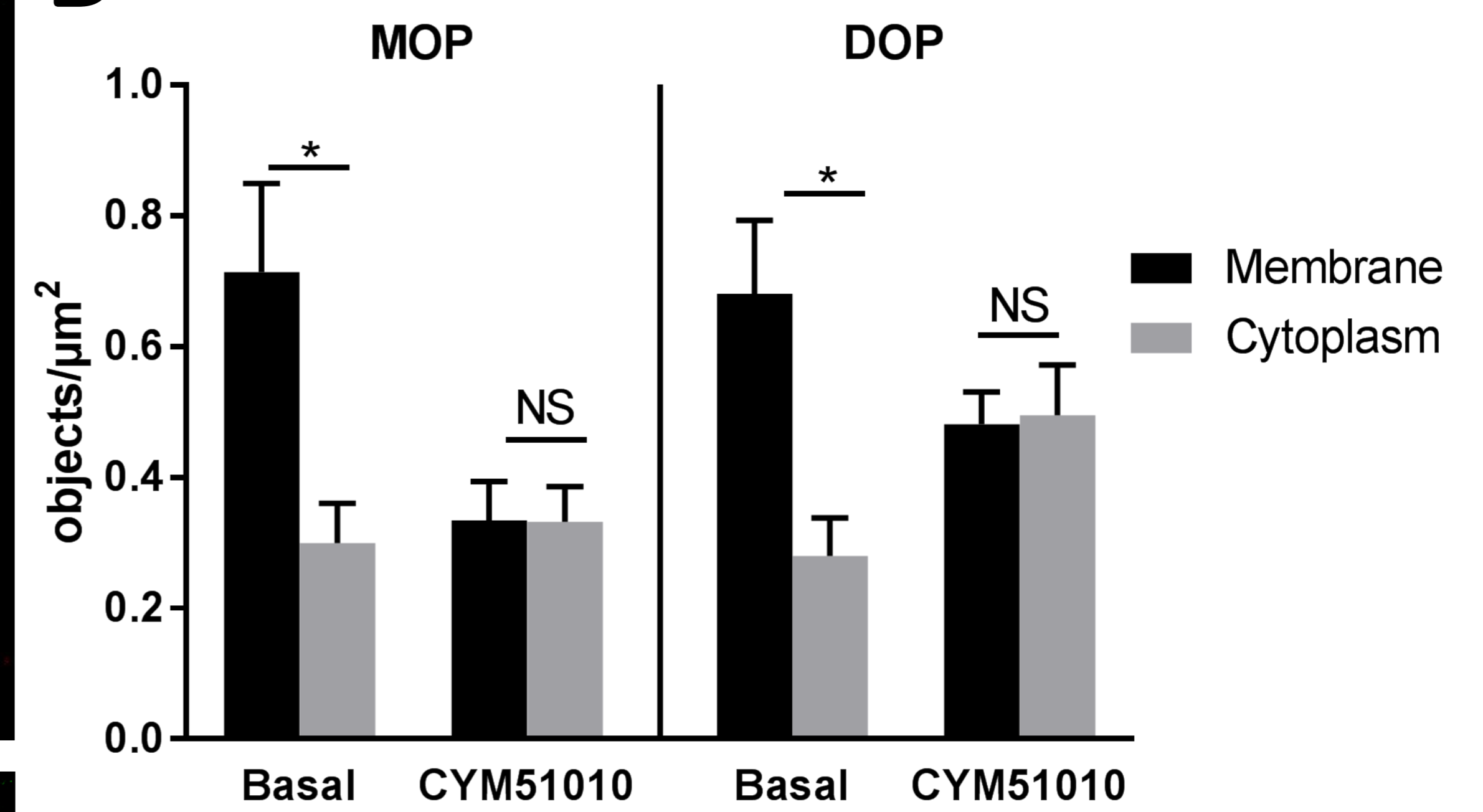
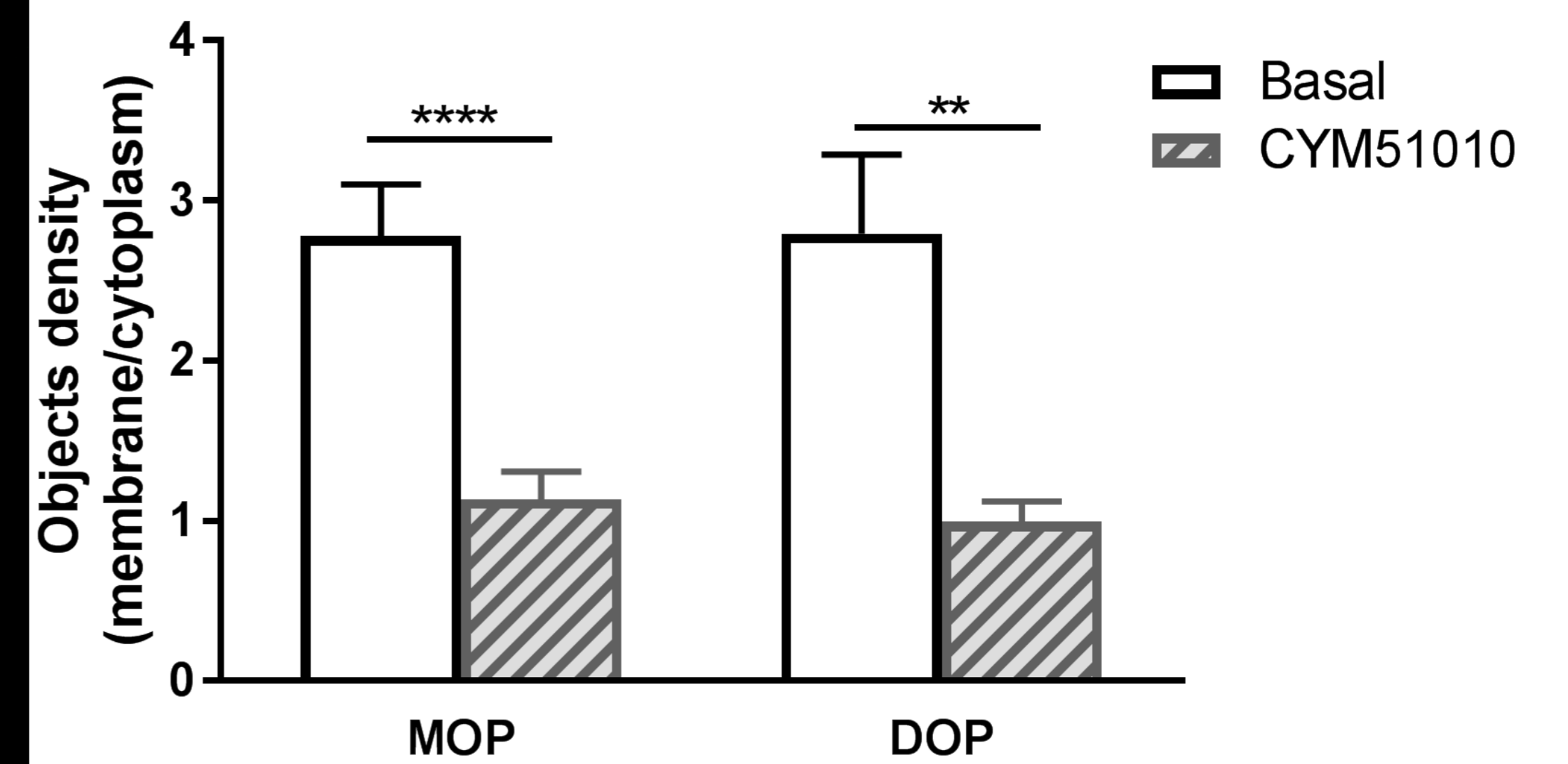
MOP-mcherry



DOP-eGFP



DAPI-MERGE

**B****C****D**